Available online at www.sciencedirect.com

ScienceDirect

Powder Technology 171 (2007) 192 – 199

POWDER TECHNOLOGY

www.elsevier.com/locate/powtec

Experimental design approach to calcium carbonate precipitation in a semicontinuous process

Marko Ukrainczyk, Jasminka Kontrec, Vesna Babić-Ivančić, Ljerka Brečević, Damir Kralj *

Laboratory for Precipitation Processes, Ruđer Bošković Institute, Bijenička cesta 54, P.O. Box 180, HR-10002 Zagreb, Croatia

Received 25 May 2006; received in revised form 29 August 2006; accepted 17 October 2006
Available online 23 November 2006

Abstract

The production of precipitated calcium carbonate, PCC, by a semicontinuous process of slaked lime carbonation was performed in a bench-scale chemical reactor, fully controlled by means of custom built electronics and software for the personal computer. Calcite crystals, with different characteristic morphologies (rhombohedral, truncated prismatic, scalenohedral, spheroidal or chain-like agglomerates) were produced by varying a range of process parameters, like temperature, supersaturation, gas mixture flow rate, stirring rate and mass concentration of $Ca(OH)_2$ suspension. In order to identify the effects of the chosen process parameters on the PCC morphology and on the related specific surface area, as well as on the extent of CO_2 conversion, an empirical approach based on the experimental design techniques was employed. A multiple correlation analysis of the obtained data suggests that temperature and conductivity significantly influence the PCC morphology, while CO_2 conversion is principally influenced by stirring rate, conductivity and gas mixture flow rate.

Keywords: Precipitated calcium carbonate (PCC); Slaked lime; Carbonation; Experimental design techniques; Multiple correlation analysis; Morphology

1. Introduction

Precipitated calcium carbonate (PCC) has received significant attention in recent years owing to its wide application in the areas of papermaking, rubber, plastics, paints, pharmacy, etc. Such a variety of applications require a PCC to have different physical and chemical properties, among which particle size, specific surface area, morphology and chemical purity are the most important.

Calcium carbonate forms different hydrates (calcium carbonate monohydrate, calcium carbonate hexahydrate, amorphous calcium carbonate) and three polymorph modifications (calcite, aragonite, vaterite). Because of its thermodynamic stability under standard conditions and its possibility to appear in various morphologies (rhombohedral, scalenohedral, spheroidal, etc.) calcite proves to be the most important polymorph in industrial application. For instance, scalenohedral calcite is used in paper and paints industry, while ultrafine rhombohedral calcite, with high specific surface area, is applied in plastics and sealants industry. Both natural (limestone, marble, chalk and coral) and synthetic (precipitated) calcium carbonate are commonly used. Natural ground calcium carbonate, obtained by mechanical treatment of minerals, often does not meet the market demands for the high quality of product. To meet these needs, calcium carbonate should be prepared under carefully controlled conditions. Only PCC can give a product with the characteristics required, as it is precipitated under controlled conditions which provide plenty of possibilities of yielding the product with predetermined properties.

PCC can be synthesized via the solution (liquid–liquid–solid) or the carbonation (gas–liquid–solid) route. The first route is often adopted in laboratory study, because of the easiness in controlling process variables. In this way, for example, Kitamura et al. [1] revealed the effect of supersaturation, feeding rate and temperature on the morphology and crystallization of polymorphs in $CaCl_2$–Na_2CO_3 aqueous solutions. The effect of inorganic additives on the physical and chemical properties of precipitates from $Ca(OH)_2$–H_2CO_3 aqueous solutions [2,3] and the conversion kinetics of vaterite to calcite in $CaCl_2$–Na_2CO_3 aqueous solutions [4] were also studied. However, the most often used route in industrial calcium

---

* Corresponding author.
E-mail address: kralj@irb.hr (D. Kralj).

0032-5910/$ - see front matter © 2006 Elsevier B.V. All rights reserved.
doi:10.1016/j.powtec.2006.10.046

carbonate synthesis is carbonation. This is due to the availability of raw materials and their low costs. The procedure consists of bubbling CO_2 gas through an aqueous $Ca(OH)_2$ suspension in a batch reactor [5].

The most common morphologies of precipitated calcite, obtained via solution and carbonation routes, are rhombohedral and scalenohedral, respectively. Calcite crystals of morphology diverse from the scalenohedral shape can be obtained in the carbonation process by addition of various additives, which affect the particle morphology and size by modifying the precipitation mechanism [6,7]. Morphological control of calcite crystals can also be achieved without use of additives. Jung et al. [8] precipitated rhombohedral and scalenohedral shape of calcite in continuous mode by using filtered solutions of $Ca(OH)_2$ and pure CO_2 gas under ‘stoichiometric’ and ‘non-stoichiometric’ conditions, respectively. To obtain the morphological change from scalenohedral to rhombohedral, García-Carmona et al. [9,10] proposed an adjustment of electrical conductivity during the semicontinuous carbonation of $Ca(OH)_2$ suspension. The explanation of such a morphological change was given in terms of the increase of both the supersaturation and the calcium to carbonate ratio in solution [10].

In the present work, the semicontinuous production of PCC in the $Ca(OH)_2(s)–CO_2(g)–H_2O$ system was studied systematically, using a bench-scale reactor. The multiphase precipitation system, in which solid, liquid and gaseous reactants and products are involved, is highly complex and difficult to model, owing to a number of physical–chemical processes taking place simultaneously. In this case, the role of phase interfaces (solid–liquid, gas–liquid, gas–solid) is of particular importance, because mass transfer, as well as heterogeneous nucleation or epitaxial growth, can occur. Therefore, we applied an empirical approach using experimental design techniques to determine the effects of process parameters (like conductivity, temperature, CO_2 flow rate, stirring rate and mass concentration of $Ca(OH)_2$ suspension) on either the specific surface area of PCC or the extent of CO_2 conversion. Such an approach and the multiple correlation analysis of the results obtained can substantially speed up even the optimization of the large scale PCC production process.

2. Experimental

2.1. Experimental set-up

A thermostatted bench-scale glass reactor of 6.0 dm^3 total volume capacity was constructed. Fig. 1 shows a line diagram of the experimental set-up. In order to achieve optimal hydrodynamic conditions in the reactor, the ratio of the liquid level to the inner vessel reactor diameter (*D*) was within the range from 1.0 to 1.5, as proposed for industrial stirred tank precipitators. Stirring was performed by a 45° pitched-blade turbine with the diameter *D*/3. The turbine was placed *D*/3 from the bottom of the inner vessel. In order to improve mixing and to prevent the vortex formation during stirring, the vessel was fitted with four vertical baffle plates of *D*/12 in width. The usual accumulation of particles in the baffle/vessel junctions was prevented by leaving narrow gaps between the baffles and the vessel wall, so that a free flow of suspension was possible. Gas was introduced into the vessel through the baffles, at the bottom of each being a nozzle of 0.7 mm in diameter. The reactor was equipped with a conductivity cell connected to the conductivity meter

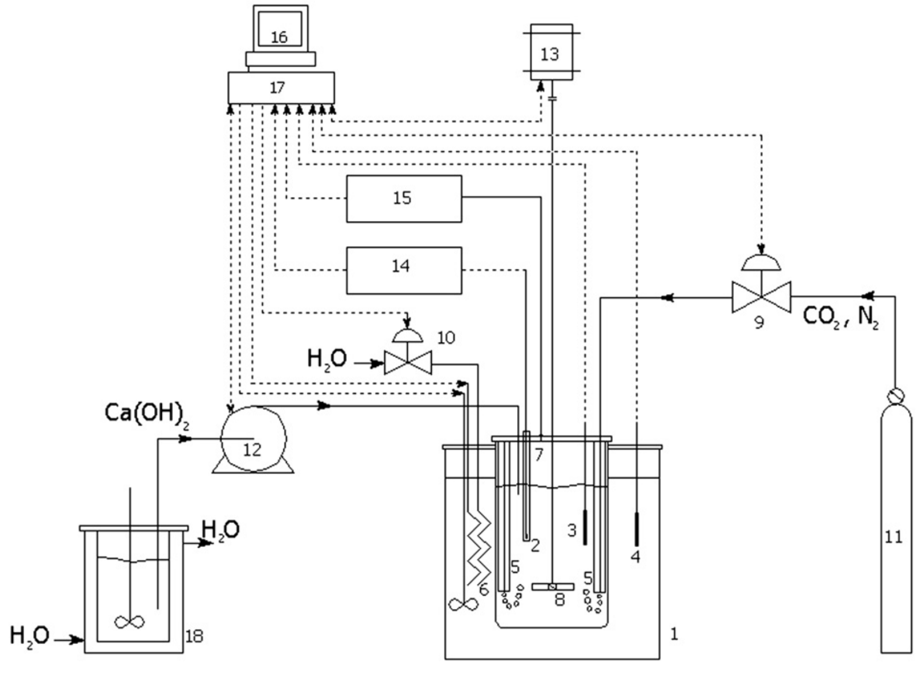

Fig. 1. Line diagram of the experimental set-up: (1) thermostatted reactor, (2) conductivity cell, (3, 4) digital temperature sound, (5) baffles with nozzle for gas injection, (6) heater and cooler, (7) gas outlet, (8) 45° pitched-blade turbine, (9) regulation valve, (10) magnetic valve, (11) gas supply bottle, (12) peristaltic pump, (13) mixing motor, (14) conductivity meter, (15) CO_2 analyser, (16) personal computer provided with control software, (17) controller, (18) thermostatted feeding tank.

(Radiometer, CDM 230), a digital carbon dioxide analyser (Quantek Instruments, 906 CO_2 Analyzer), digital temperature sensors, a flow meter (Cole Parmer) calibrated for 20% CO_2/80% N_2 (v/v), a regulation valve for the continuous gas flow control (Aalborg), a peristaltic pump (Cole Parmer, Masterflex L/S), a stirrer and a thermostatted feeding tank of 2 dm^3 volume capacity. Process parameters (conductivity, temperature, CO_2 flow rate and rate of stirring) were continuously measured by means of a home-made data acquisition system and an electronic controller connected to the PC.

2.2. Experimental procedure

Initially, the reactor was filled with 3.0 dm^3 of deionized water. After reaching the predetermined working temperature (θ), deionized water was stirred at a maximum stirring rate (n) of 1400 min^{-1} and presaturated by gas mixture of 20% CO_2/80% N_2 (Inertal 20, Messer) at a maximum gas flow rate $Q(CO_2) = 5.0$ dm^3 min^{-1}. The saturation, detected as a constant conductivity, was usually obtained after approximately 1 min. A number of carbonation experiments were performed by varying the process parameters within the predetermined ranges: flow rate of the gas mixture, 1.0 dm^3 $min^{-1} < Q < 5.0$ dm^3 min^{-1}; stirring rate, 800 $min^{-1} < n < 1400$ min^{-1}; mass concentration of $Ca(OH)_2$ suspension, 50 g $dm^{-3} < \gamma < 150$ g dm^{-3}; and conductivity, 1.0 mS $cm^{-1} < \kappa_{25} < 7.0$ mS cm^{-1} (refers to 25 °C). The apparently constant supersaturation was maintained in each experiment of this semicontinuous process. For this purpose, the conductivity was controlled and kept at the predetermined value by feeding the reactor with the thermostatted $Ca(OH)_2$ suspension ($Q_{max}(Ca(OH)_2) = 280$ cm^3 min^{-1}), using the Proportional-Integral-Derivative (PID) regulation for the peristaltic pump. The flow of the $Ca(OH)_2$ suspension was usually stopped 15 min after starting the experiment, while the gas flow was kept constant until the endpoint of the carbonation reaction, which was indicated by a drop of conductivity.

The volume fraction of CO_2, $\varphi(CO_2)$, was continuously measured during the carbonation reaction, so that the CO_2

Table 1
Experimental matrix for *D*-optimal design and results

Trial	Independent variables					Results				
	θ(a) (°C)	κ_{25}(b) (mS cm^{-1})	$\gamma(Ca(OH)_2)$(c) (g dm^{-3})	n(d) (min^{-1})	$Q(CO_2)$(e) (dm^3 min^{-1})	$X(CO_2)$(f) (%)	m(g) (g)	s(h) (m^2 g^{-1})	Morphology(i)	d_m(j) (μm)
1	20	1	50	800	3	43.7	24	2.1	R	0.5
2	20	1	50	800	5	45.8	27	2.2	R	0.5
3	20	1	50	1100	3	57.5	28	2.2	R	0.5
4	20	1	50	1400	1	67.3	24	2.3	R	0.5
5	20	1	100	1400	1	71.3	24	1.7	R	0.5
6	20	1	150	800	1	42.2	13	2.2	R	0.5
7	20	1	150	1100	5	41.5	34	2.2	R	0.5
8	20	1	150	1400	5	62.9	39	2.3	R	0.5
9	20	4	100	800	3	40.4	40	17.2	CL	1.0
10	20	7	50	800	1	60.0	28	24.8	S	0.03
11	20	7	50	1400	1	87.6	48	24.2	S	0.03
12	20	7	50	1400	5	54.6	107	24.3	S	0.03
13	20	7	150	800	5	33.8	98	27.0	S	0.02
14	20	7	150	1100	3	65.1	46	29.3	S	0.02
15	20	7	150	1400	1	85.5	81	26.7	S	0.03
16	35	1	100	800	5	40.4	32	2.2	R	1.0
17	35	1	150	1100	1	59.7	19	2.2	R	1.0
18	35	4	50	1400	1	80.1	32	2.6	TP, R	1.0
19	35	4	100	1100	3	64.4	47	4.5	TP	1.0
20	35	4	150	1400	3	67.6	49	4.0	TP	1.0
21	35	7	100	1100	3	70.9	55	7.4	Sc	1.0
22	50	1	50	800	1	44.3	13	2.6	R	1.5
23	50	1	50	1400	5	55.3	45	2.4	R	1.5
24	50	1	100	1400	5	55.4	57	1.1	R	2.0
25	50	1	150	800	3	38.7	18	2.1	R	1.5
26	50	1	150	800	5	30.2	28	2.0	R	1.5
27	50	1	150	1400	1	73.1	24	1.4	R, Sc	2, 0.5
28	50	4	50	1100	5	50.2	65	4.2	Sc, TP	1.0
29	50	4	100	1100	1	70.1	39	2.7	R, TP	1.0
30	50	7	50	800	1	58.2	26	7.8	Sc	1.0
31	50	7	50	800	5	41.5	52	8.8	Sc	1.0
32	50	7	50	1400	1	81.5	34	6.8	Sc	1.0
33	50	7	50	1400	3	74.2	63	6.1	Sc	1.0
34	50	7	150	800	1	67.5	30	7.0	Sc	1.0
35	50	7	150	1400	5	59.5	104	7.1	Sc	1.0

(a)Working temperature; (b)conductivity at 25 °C; (c)mass concentration of $Ca(OH)_2$ suspension; (d)stirring rate; (e)gas flow rate; (f)CO_2 conversion; (g)mass of precipitate; (h)specific surface area; (i)R — rhombohedral, CL — chain-like, S — spherical, TP — truncated prismatic, Sc — scalenohedral; (j)particle dimension.

conversion, $X(CO_2)$, was calculated at any moment of the reaction according to the equation:

$$X(\mathrm{CO_2}) = 100\cdot[(\varphi_0(\mathrm{CO_2}) - \varphi(\mathrm{CO_2}))/\varphi_0(\mathrm{CO_2})],$$

by using the known initial volume fraction, $\varphi_0(CO_2)=0.2$.

At the end of each experiment, an aliquot (200–400 cm^3) of the final suspension was taken and the precipitate was separated by treating the sample in a centrifuge for 10 min, n_c= 4000 min^{-1}. The precipitate was dried at 105 °C for 3 h and weighed in order to estimate the yield of the reaction. The composition of the solid phase was determined by Fourier transform infrared, FT-IR, spectroscopy (Mattson, Genesis Series). The size and morphology of particles were observed using transmission electron microscopy, TEM (FEI, Morgagni 268 D) and the specific surface area, *s*, was determined using the multiple BET method (Micromeritics, Gemini) with nitrogen gas as the adsorbate.

2.3. Experimental design and statistical analysis

Experimental design techniques were used to identify the effects of temperature, conductivity, flow rate of gas mixture, stirring rate and mass concentration of suspension on the physical–chemical properties of PCC and on CO_2 conversion. Based on the *D*-optimal algorithm [11], an optimally designed matrix of 35 experiments was chosen from the possible 243 experiments. The *D*-optimal experimental domain and the results gained are shown in Table 1. Modelling was aimed at describing both the specific surface area of the PCC obtained and the conversion of CO_2 as a function of the independent variables of the *D*-optimal design. This model permitted the evaluation of the effects of linear, quadratic and interactive terms of the independent variables on the chosen dependent variables. The experimental design and statistical analysis were performed using STATISTICA 6.0 (StatSoft, USA).

3. Results and discussion

The experimental conditions and the results of the semi-continuous PCC production in a bench-scale reactor are given in Table 1. The supersaturation (conductivity, κ_{25}), the temperature, the CO_2 flow rate, the stirring rate and the mass concentration of $Ca(OH)_2$ suspension are chosen, among the other process parameters, as the most relevant for determining the physical–chemical properties of PCC and the reactant (CO_2) conversion. These process parameters were applied in the ranges that assumed a significant yield of PCC, possibly the optimal in a bench-scale production.

The results of mineralogical analyses of the final products show that calcite was the only $CaCO_3$ polymorph obtained at the end of each carbonation experiment. The morphology was found to be rhombohedral (R), scalenohedral (Sc), spheroidal (S) or truncated prismatic (TP). However, even a superficial analysis reveals that the morphology and size distribution of particles are influenced mostly by the temperature and supersaturation (conductivity) of the system. On the other hand, for the applied ranges of other parameters, i.e. the CO_2 flow rate, the stirring rate and the mass concentration of $Ca(OH)_2$ suspension, no noticeable influence on the selected properties of

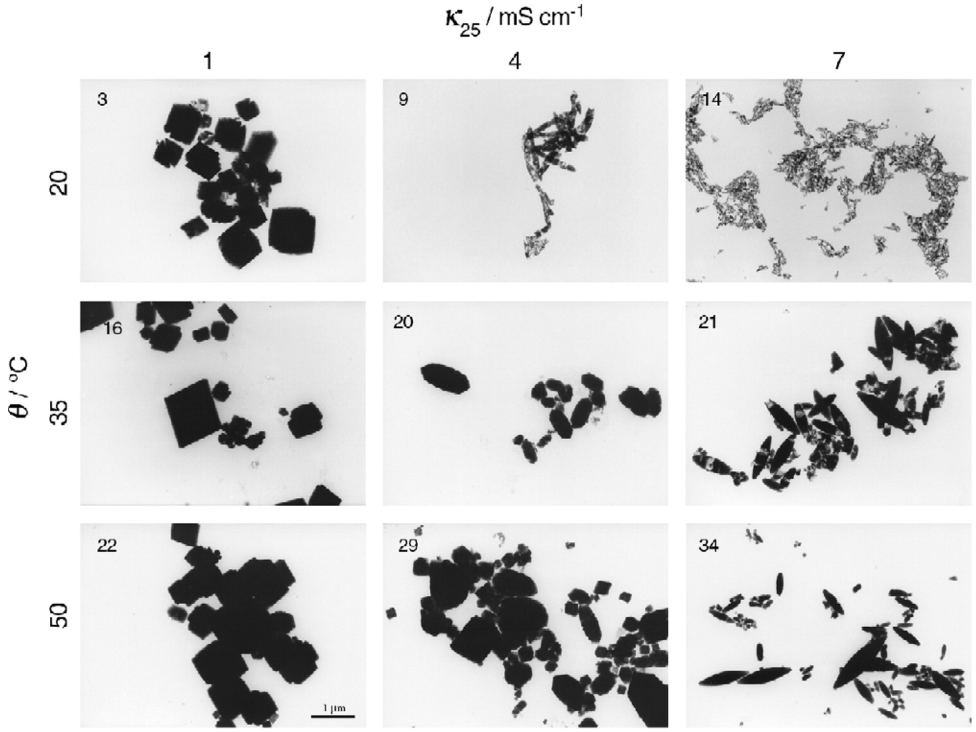

Fig. 2. TEM micrographs of PCC produced at different temperatures (θ=20; 35 and 50 °C) and conductivities (κ_{25}=1.0; 4.0 and 7.0 mS cm^{-1}). All micrographs have equal magnification, bar=1 μm. Numbers denote trials from Table 1.

the system was observed. Fig. 2 shows typical TEM microphotographs of PCC obtained at different temperatures and conductivities. It is evident that the size of crystals produced at $\theta=50$ °C varied in the range from approximately 0.3 μm to 1.5 μm, while their morphologies were either rhombohedral ($\kappa_{25}=1.0$ mS cm^{-1}) or mixtures of rhombohedral and truncated prismatic ($\kappa_{25}=4.0$ mS cm^{-1}) or scalenohedral ($\kappa_{25}=7.0$ mS cm^{-1}). Similar behaviour was observed in the experiments at $\theta=35$ °C, whereas at $\theta=20$ °C, crystalline, rhombohedral, products were obtained only at the lowest supersaturation ($\kappa_{25}=1.0$ mS cm^{-1}). At higher conductivities ($\kappa_{25}=4.0$ mS cm^{-1} and $\kappa_{25}=7.0$ mS cm^{-1}) PCC appeared in the form of submicrometric "chain-like" (CL) elongated agglomerates or as nanometric spheroidal particles, $d_m \approx 30$ nm. The morphologies described here are similar to those reported by Garcia-Carmona et al. [9,10], differing only by the appearance of truncated prismatic crystals obtained in our experiments at $\theta \geq 35$ °C and $\kappa_{25}=4.0$ mS cm^{-1}. However, such morphology was observed in our previous work [2], in which the precipitation was initiated by mixing calcium hydroxide and carbonic acid solutions in the presence of magnesium salts.

It is interesting to note that a relation between the morphology of calcite crystals and the measured specific surface area, s, was obtained (see Table 1). Thus, the s-values of rhombohedral calcites were found to be approximately $s=2$ m^2 g^{-1}, of truncated prismatic $s=4$ m^2 g^{-1}, of scalenohedral $s=7$ m^2 g^{-1}, of chain-like $s=17$ m^2 g^{-1} and of spheroidal $s=25$ m^2 g^{-1}. The mean PCC particle size, d_m, estimated using TEM, was found to be in the range from 0.02 to 2 μm.

As has already been suggested by other authors [10], the morphology of particles is a consequence of the mechanism of their formation. Therefore, it is to be expected that the particle morphology can be anticipated from the shape of progress curves, κ_{25} vs. time. Fig. 3 shows typical progress curves (κ_{25} vs. time and $\varphi(CO_2)$ vs. time) during the semicontinuous process of slaked lime carbonation at $\kappa_{25}=7.0$ mS cm^{-1} and different temperatures (Table 1, trials 12, 21 and 30). The initial, ascending, part of the κ_{25} vs. time curves corresponds to the simultaneous dissolution of $Ca(OH)_2$ and CO_2. The CO_2 gas was continuously fed into water, previously saturated with CO_2, at a constant high flow rate, in order to keep the set-point value, $\kappa_{25}=7.0$ mS cm^{-1}. After reaching this predetermined κ_{25} value, the flow rate of $Ca(OH)_2$ suspension was maintained constant (conductivity plateau) by means of the PID regulation. Simultaneously with the initial increase of κ_{25}, the $\varphi(CO_2)$ vs. time curves show a rapid decrease, as a consequence of CO_2 consumption in the process of calcium carbonate precipitation. The addition of $Ca(OH)_2$ suspension was stopped after 15 min, while the flow of the gas mixture was further kept constant, in order to complete the precipitation of the excess of $Ca(OH)_2$ (Fig. 3, $\theta=35$ °C and $\theta=50$ °C). During this part of the process, κ_{25} decreases and its minimum value indicates the end of the calcium carbonate formation. A subsequent increase of κ_{25} is a consequence of PCC dissolution in the excess of carbonic acid that remained in the system. The shape of the κ_{25} vs. time curve of the experiment carried out at $\theta=20$ °C differs somewhat from the other temperatures, since the conductivity suddenly increases after a period of apparently constant value ($\kappa_{25}=7.0$ mS cm^{-1}) and reaches the value of about 8.6 mS cm^{-1}. Such behaviour during the process of the PCC formation in a semicontinuous reactor was explained by García-Carmona et al. [10,12] as a consequence of nucleation and growth of a certain calcium carbonate precursor phase, probably an amorphous calcium carbonate, on the surfaces of suspended $Ca(OH)_2$ particles. Since the precursor is extremely unstable [13], it rapidly dissolves during its transformation into stable calcite, thus liberating the surfaces of $Ca(OH)_2$ particles and causing the uncontrolled increase of conductivity. Similar behaviour was also observed in experiments in which κ_{25} was maintained at the value of 4.0 mS cm^{-1}.

In order to confirm the decisive role of the excess of suspended $Ca(OH)_2$, rather than the role of temperature, on the

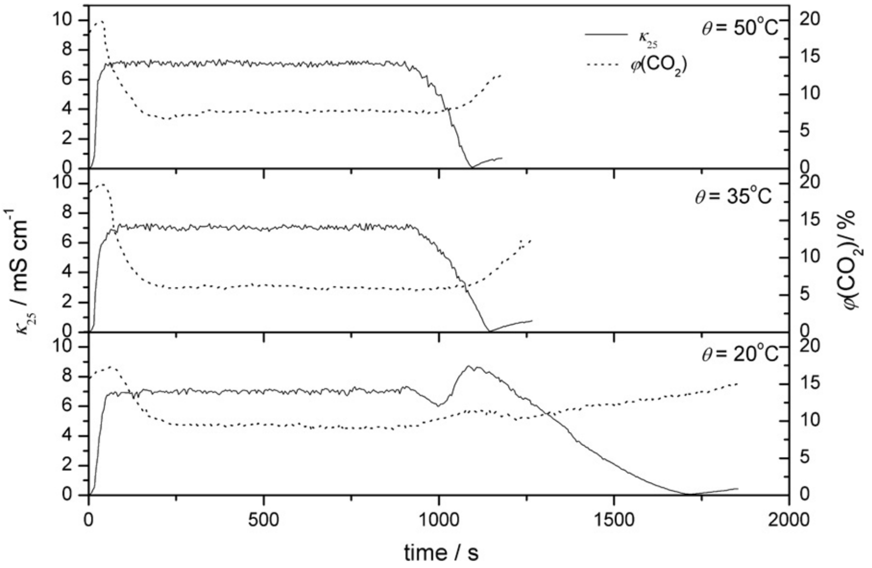

Fig. 3. Typical progress curves of conductivity (κ_{25}) and volume fraction of CO_2, ($\varphi(CO_2)$) during the process of carbonation performed at $\kappa_{25}=7.0$ mS cm^{-1} and different temperatures ($\theta=20$; 35 and 50 °C).

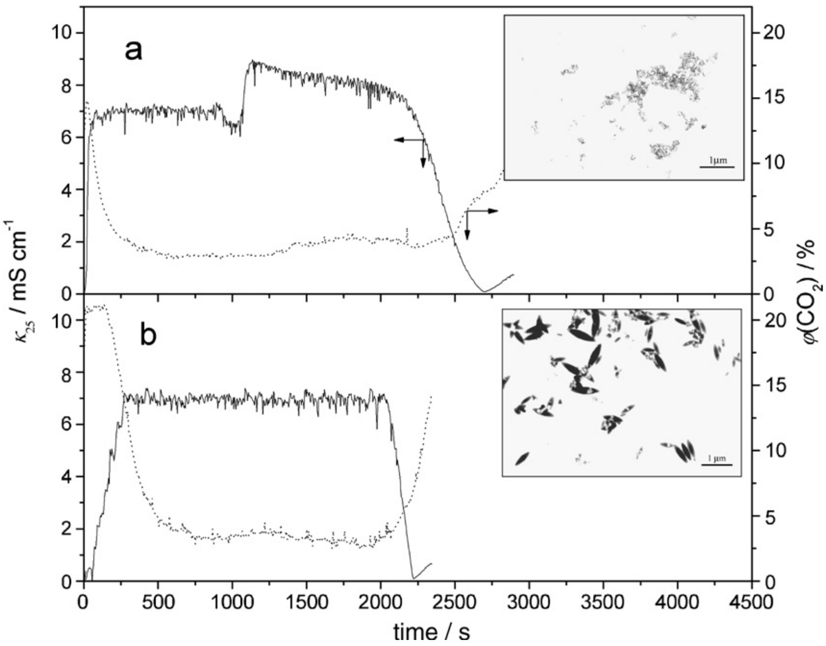

Fig. 4. Progress curves obtained during the carbonation process (θ=20 °C, κ_{25}=7.0 mS cm^{-1}, Q(CO$_2$)=1.0 dm^3 min^{-1}, $Q_{\max}$(Ca(OH)$_2$)=280 cm^3 min^{-1}, γ(Ca(OH)$_2$)=150 g dm^{-3}, n=1400 min^{-1}) in which the precursor phase was formed (a) and in which the carbonation process was carried out under the same experimental conditions, but applying a slow addition of Ca(OH)$_2$ suspension ($Q_{\max}$(Ca(OH)$_2$=40 cm^3 min^{-1}) during the set-point adjustment at the beginning of the process (b). TEM micrographs of the corresponding PCC particles are represented.

process of the formation of specific PCC morphologies and their specific surface areas as well, additional experiments were performed. In these experiments, the values of the process parameters were varied beyond the ranges shown in Table 1. Fig. 4a shows a typical progress curve of the carbonation process, in which the precursor phase is formed. The figure also shows a TEM image of the spheroidal particles, obtained at the end of this process, with a high specific surface area (s=28 m^2 g^{-1}). Under the same experimental conditions (θ=20 °C, κ_{25}=7.0 mS cm^{-1}, Q(CO$_2$)=1.0 dm^3 min^{-1}, γ(Ca(OH)$_2$)=150 g dm^{-3}, n=1400 min^{-1}), but applying a slow addition of Ca(OH)$_2$ suspension ($Q_{\max}$(Ca(OH)$_2$=40 cm^3 min^{-1}) during the set-point adjustment at the beginning of the process (κ_{25}=7.0 mS cm^{-1}), the progress curve remains constant even after

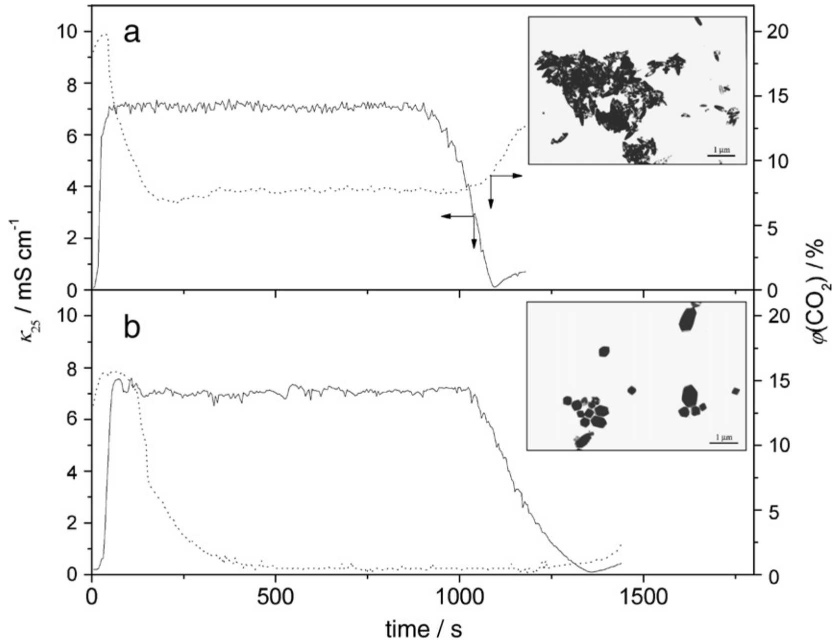

Fig. 5. Progress curves and TEM micrographs of the corresponding calcite particles obtained by adjusting the gas flow rate, under the otherwise identical conditions (θ=50 °C, κ_{25}=7.0 mS cm^{-1}, n=1400 min^{-1}, γ(Ca(OH)$_2$)=150 g dm^{-3}): (a) higher gas flow rate, Q(CO$_2$)=5.0 dm^3 min^{-1} and (b) lower gas flow rate, Q(CO$_2$)=0.3 dm^3 min^{-1}.

Table 2
Final equations in terms of transformed variables

Response	Equation		R^2	R^2_{adj}
s (m^2 g^{-1})	$s=7.652-4.930\theta-2.573\theta^2+5.690\kappa-4.656\theta\kappa-2.4550\theta^2\kappa$	(1)	0.985	0.982
$X(CO_2)$ (%)	$X(CO_2)=57.515+4.564\kappa+11.513n-8.985Q(CO_2)-3.619\kappa Q(CO_2)$	(2)	0.922	0.912

30 min (Fig. 4b). The corresponding precipitate consisted of micrometric scalenohedral particles, with a significantly lower specific surface area of $s=9.5$ m^2 g^{-1}. The properties of PCC produced in this way are the result of the non-existence of any accumulated solid $Ca(OH)_2$ in the system during carbonation. Namely, owing to the slow initial addition of $Ca(OH)_2$ slurry, the dissolution of $Ca(OH)_2$ particles is much faster than the formation of PCC.

It is generally known that switching between the predominantly scalenohedral to rhombohedral morphology of the precipitated calcite crystals is determined by the ratio of total dissolved calcium to carbonate species, $[Ca]_{tot}/[CO_3]_{tot}$. Thus, García-Carmona et al. [10] suggest that at higher conductivities and temperatures >25 °C, predominantly scalenohedral crystals form because of the higher $[Ca]_{tot}/[CO_3]_{tot}$ ratio, which is a consequence of the higher concentration of dissolved $Ca(OH)_2$. Fig. 5 shows that, by adjusting the gas flow rate, under the otherwise identical conditions ($\theta=50$ °C, $\kappa_{25}=7.0$ mS cm^{-1}, $n=1400$ min^{-1}, $\gamma(Ca(OH)_2)=150$ g dm^{-3}), either scalenohedral or rhombohedral calcite particles can precipitate. The higher gas flow rate, $Q(CO_2)=5.0$ dm^3 min^{-1}, creates conditions for scalenohedral particles ($s=7.0$ m^2 g^{-1}) to be produced (Fig. 5a), since larger amounts of CO_2 can be dissolved. On the other hand, when $Q(CO_2)=0.3$ dm^3 min^{-1}, a mixture of truncated prismatic and rhombohedral calcite crystals ($s=4.0$ m^2 g^{-1}) is formed (Fig. 5b). It is also evident that at lower $Q(CO_2)$ a lower $\varphi(CO_2)$ was achieved, as it is to be expected.

In order to be able to explain and quantitatively describe the relationship between the selected responses (specific surface area of PCC and conversion of CO_2) and the independent variables, the empirical models were proposed. Linear, quadratic and interactive terms were considered in these models. Independent variables were linearly transformed into values between −1 and +1, to correctly perform the multiple correlation analysis. In this way, the estimated effects (regression coefficients) were comparable in size. The number of experiments performed (35 from 243 possible) seems to be a good compromise between the large number of experiments that gives better resolution of the empirical model predicting the properties of PCC and the practical requirement for prompt optimization process of large scale PCC production. However, the number of experiments performed in this work is much higher than the number of experiments performed in the systems of similar complexity: for example, 19 experiments were performed, from possible 2916, in order to predict the formation of spherulitic $CaCO_3$ [14]. The statistical significance of the regression coefficients was determined by the variance analysis (ANOVA). The terms having ANOVA p-values lower than 0.05 (95% level of significance) were added to the model. Final equations, Eq. (1) and Eq. (2), including the significant terms only, are given in Table 2. Their coefficient of determination, R^2, and the adjusted coefficient of multiple determinations, R^2_{adj}, are also represented. The values of R^2 and R^2_{adj} for the specific surface area and $X(CO_2)$ were higher than 0.98 and 0.91,

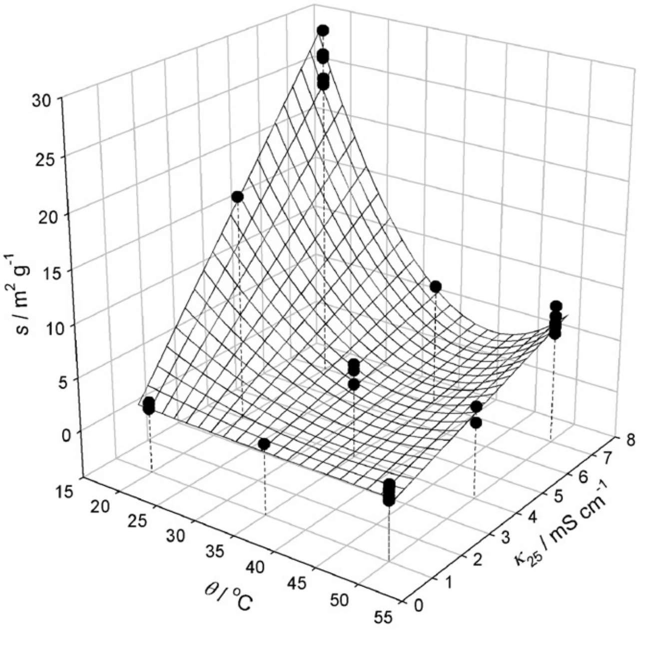

Fig. 6. Specific surface area (s) of PCC as a function of temperature (θ) and conductivity (κ_{25}). Circles denote the experimental data.

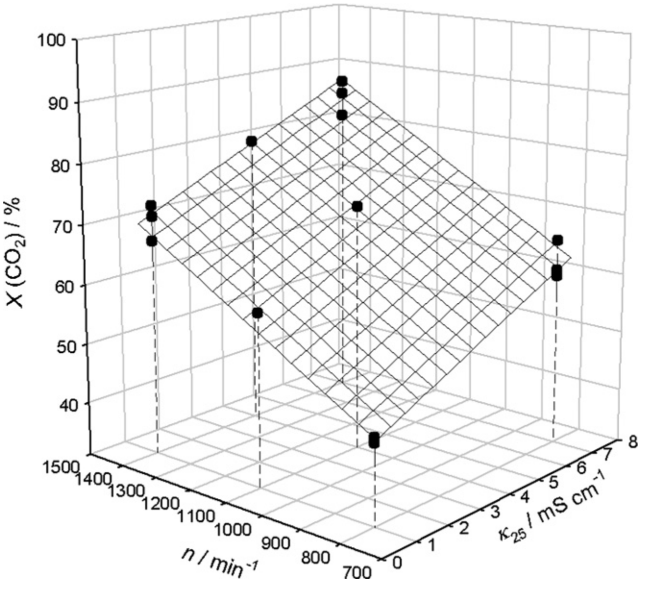

Fig. 7. Conversion of CO_2 (X) as a function of stirring rate (n) and conductivity (κ_{25}) at a CO_2 flow rate of 1 dm^3 min^{-1}. Circles denote the experimental data.

respectively, indicating that the models were adequate to explain the variability in the experimental data.

It is evident from Eq. (1) and the 3-D surface plot obtained from this model (Fig. 6), that the specific surface area depends on temperature and conductivity. The negative linear coefficient and the quadratic coefficient of θ indicate that the specific surface area increases with decreasing temperature, while the positive linear coefficient of κ_{25} indicates that the specific surface area increases with increasing conductivity. The obtained interactive terms could be explained by a well-known effect of temperature on the concentration of dissolved electrolytes, expressed as the change in conductivity.

The results of the multiple correlation analysis, concerning the effects of the process parameters on CO_2 conversion, are represented by Eq. (2). By comparing the magnitude of the coefficients, it is evident that the effect of stirring is stronger than the effects of the gas mixture flow rate and of conductivity. However, the positive linear coefficient of n and κ_{25} contribute to the increase of $X(CO_2)$, whereas the negative linear coefficient of $Q(CO_2)$ has a reverse trend on $X(CO_2)$. Since it is shown that the flow rate of CO_2 has no significant effect on the specific surface area of particles, it can be deduced that the minimum value of the gas flow rate, $Q(CO_2) = 1.0\ \mathrm{dm}^3\ \mathrm{min}^{-1}$, is optimal for the given investigations. The respective graphical presentation of the effects of stirring rate and conductivity on the conversion of CO_2, at the optimum flow rate of $1.0\ \mathrm{dm}^3\ \mathrm{min}^{-1}$, is shown as the 3-D surface plot in Fig. 7. The highest values of CO_2 conversion were obtained at the highest stirring rates and conductivities. Under such conditions, the conversion is facilitated by the enhanced gas dispersion and mass transfer of CO_2 into solution, as well as by the enhanced CO_2 solubility at higher pH, the latter being a consequence of the higher concentration of dissolved $Ca(OH)_2$, which is expressed as an increase in conductivity.

4. Conclusions

The production of precipitated calcium carbonate, PCC, by a semicontinuous process of slaked lime carbonation was performed in a bench-scale chemical reactor equipped with a number of sensors and actuators. The carbonation process was PID regulated and fully controlled by means of custom built electronics and software for the personal computer.

It has been demonstrated that, for the chosen range of process parameters (temperature, supersaturation, gas mixture flow, stirring rate and mass concentration of $Ca(OH)_2$ suspension), calcite particles/crystals with different characteristic morphologies (rhombohedral, truncated prismatic, scalenohedral or chain like agglomerates) can be produced. Because of a large number of physical–chemical processes, taking place simultaneously during the carbonation (CO_2 and $Ca(OH)_2$ dissolution, heterogeneous and homogeneous nucleation of $CaCO_3$, spontaneous or epitaxial crystal growth), it is difficult to give an exact prediction of the PCC properties. A large number of experiments are needed in order to obtain the product of desired properties.

Therefore, an empirical approach based on the experimental design techniques was employed to identify the effects of the chosen process parameters on the PCC morphology (specific surface area) and on the extent of CO_2 conversion. For this purpose, an optimally designed matrix consisting of 35 experiments was chosen from the possible 243.

A multiple correlation analysis of the obtained data suggests that temperature and conductivity significantly influence the PCC morphology. At low temperatures and high conductivities, submicrometric PCC with a high specific surface area can be produced, whereas at high temperatures and low conductivities well-crystallized micrometric calcite of low specific surface area precipitates.

The stirring rate, conductivity and the gas mixture flow rate have been found to be mostly responsible for CO_2 conversion into calcium carbonate, at the given experimental (process) parameters.

It is also shown that, even at low temperatures and high conductivity (supersaturation), a well-crystallized PCC of low specific surface area can be produced by applying a very slow addition rate of $Ca(OH)_2$ suspension at the beginning of the carbonation process. These results emphasize the role of solid–liquid phase interface on the physical chemical properties of precipitate and the complexity of such multiphase precipitation system, in which solid, liquid and gaseous reactants and products are involved.

Acknowledgements

We thank Dr. Sc. Nikola Ljubešić for the TEM analysis. This research has been sponsored by the Ministry of Science, Education and Sport of the Republic of Croatia (project No. TP 01/0098-30).

References

[1] M. Kitamura, J. Cryst. Growth 237–239 (2002) 2205–2214.
[2] D. Kralj, J. Kontrec, Lj. Brečević, G. Falini, V. Nothig-Laslo, Chem. Eur. J. 10 (2004) 1647–1656.
[3] J. Kontrec, D. Kralj, Lj. Brečević, G. Falini, S. Fermani, V. Nothig-Laslo, K. Mirosavljević, Eur. J. Inorg. Chem. (2004) 4579–4585.
[4] D. Kralj, Lj. Brečević, J. Kontrec, J. Cryst. Growth 177 (1997) 248–257.
[5] P.C. Chen, C.Y. Tai, K.C Lee, Chem. Eng. Sci. 52 (1997) 4171.
[6] J. García-Carmona, J. Gómez-Morales, J. Fraile-Sáinz, R. Rodríquez-Clemente, Powder Technol. 130 (2003) 307–315.
[7] L. Xiang, Y. Xiang, Z.G. Wang, Y. Lin, Powder Technol. 126 (2002) 129–133.
[8] W.M. Jung, S.H. Kang, W.S. Kim, C.K. Choi, Chem. Eng. Sci. 55 (2000) 733.
[9] J. García-Carmona, J. Gómez-Morales, R. Rodrígrez-Clemente, J. Colloid Interface Sci. 216 (2003) 434–440.
[10] J. García-Carmona, J. Gómez-Morales, R. Rodrígrez-Clemente, J. Cryst. Growth 249 (2003) 561–571.
[11] StatSoft, Inc. (2003). STATISTICA (data analysis software system), version 6 and STATISTICA electronics manual, Tulsa, OK, www.statsoft.com.
[12] J. García-Carmona, J. Gómez-Morales, J. Fraile-Sáinz, E. Loste, R. Rodríguez-Clemente, J. Cryst. Growth 262 (2004) 479–489.
[13] Lj. Brečević, A.E. Nielsen, J. Cryst. Growth 98 (1989) 504–510.
[14] S.L. Tracy, C.J.P. François, H.M. Jennings, J. Cryst. Growth 193 (1998) 374–381.